The effectiveness of patch repairs to restore the impact properties of carbon-fibre reinforced-plastic composites

Z.E.C. Hall [a,*], J. Liu [a], R.A. Brooks [a], H. Liu [a,*], J.W.M. Crocker [a], A.M. Joesbury [b], L.T. Harper [b], B.R.K. Blackman [a], A.J. Kinloch [a], J.P. Dear [a,*]

[a] Department of Mechanical Engineering, Imperial College London, South Kensington Campus, London SW7 2AZ, UK
[b] Composites Research Group, University of Nottingham, University Park, Nottingham NG7 2RD, UK

A B S T R A C T

The present paper studies the low-velocity impact testing of carbon-fibre reinforced-plastic (CFRP) pristine and patch-repair CFRP panels. Firstly, the effect of repeated impacts on the pristine CFRP damage growth is considered at impact energies of 7.5, 10.5 and 30 J. Secondly, such tests lead to a single-sided, patch-repair panel being manufactured by removing a 40 mm diameter central hole, to act as the 'damaged area', from the parent CFRP panel and then adhesively-bonding a circular CFRP patch-repair over the hole so generated. Various diameters and thicknesses for the CFRP patch-repair are employed and, in some cases, a CFRP circular plug is also used to fill the hole created by removal of the parent composite. The measured load versus time, and load versus displacement, traces are compared. Further, the extent and location of any interlaminar damage, i.e. delaminations between the plies of the CFRP, caused by the impact event are mapped using an ultrasonic C-scan technique. It is shown that single-sided patch repairs can be very effective in restoring the impact performance of damaged CFRP panels.

1. Introduction

Composite materials based upon carbon-fibre reinforced-plastics (CFRPs) have been widely used in aerostructures over the last three decades mainly due to (a) their excellent strength to weight, and stiffness to weight, ratios, (b) their very good cyclic fatigue resistance and (c) the ability to control their mechanical properties by suitably changing the fibre lay-up. However, an area of particular concern when considering the performance of composite materials, such as CFRPs, for aircraft structures is the impact performance of the composite. Therefore, firstly, the initial impact performance of the pristine CFRP is of interest because there are many impact scenarios. These include impact events that may arise from dropped tools, bird strikes, hail stones, runway debris, airport equipment striking the fuselage and hard landings. Secondly, these impact events may lead to damage in the CFRP which now needs to be repaired to recover the mechanical performance of the composite material. The two most common repair techniques for composite materials are patch- and scarf-repairs and, for secondary aircraft structures, these repair methodologies involve the use of adhesive bonding as the most common joining technology used for the repair. Thirdly, obviously of great interest is the impact behaviour of the repaired composite material.

Firstly, considering the impact of CFRP panels, and other more complex structures, then this has been the subject of much research

---

[e.g. 1–12], since such composite materials are susceptible to impact damage, which may not be readily visible but which can lead to a significant loss of structural integrity. There are two major damage mechanisms observed when a CFRP composite is impacted at a relatively low-velocity which cause a loss of mechanical performance. Firstly, there is intralaminar damage which typically involves plastic deformation of the matrix, matrix cracking, fibre debonding and localised fibre failure. Secondly, there is interlaminar damage which involves the initiation and growth of delaminations, i.e. interlaminar cracking, between the layers that form the composite laminate. These two main damage mechanisms are interactive during the impact event.

Secondly, when such intralaminar and interlaminar damage needs to be repaired there are two main types of repair techniques for composite materials [13–16], namely patch- and scarf-repairs, as shown schematically in Fig. 1. In the case of secondary, non-critical structures, the repair material is typically joined to the parent composite solely via the use of adhesive-bonding techniques. (If primary, critical structures are repaired then an alternative, or additional, joining method, e.g. titanium fasteners, must be used.) Scarf repairs, see Fig. 1 (b), are often the preferred method to restore the load-bearing capacity of a composite structure, since they are associated with relatively lower stress-concentrations and are more aerodynamically efficient. However, they suffer from several disadvantages. For example, they are far more complex to manufacture and, if a relatively large patch is needed, then a great deal of undamaged composite material needs to be removed. Thus, patch repairs are also commonly used and they cover, and overlap, the damaged area and are usually thinner than the parent material, as shown schematically in Fig. 1 (a). The patch repair can be single- or double-sided, with the former type having a patch adhesively-bonded to only one side of the parent panel, as in Fig. 1 (a), and the latter type having a repair patch bonded onto both sides of the parent panel, but which is not always possible in practice. When manufacturing a patch repair, the damage can either be removed or the patch placed over the top of the damage area. If the damaged area is removed, a polymeric resin or a plug of the parent composite material may often be used to fill the hole so generated. Single-sided patch repairs, which are adhesively-bonded to the damaged parent composite material, are the focus of the present work since (a) they are widely used in repairing aerostructures, (b) they are relatively straightforward to manufacture and (c) their effectiveness can be readily assessed by impact testing of the repaired CFRP panel.

Thirdly, as mentioned above, obviously of great interest is the impact behaviour of the repaired composite material. The most common impact tests that have been undertaken on pristine and repaired composites have been conducted at a relatively low-velocity using hard impactors and some experimental and modelling research [17–21] has been reported. For example, Coelho et al. [18] tested single-sided, glass-fibre reinforced-plastic (GFRP) patch repairs which had been adhesively-bonded to GFRP parent panels and subjected the repairs to impact tests, using impact energies from 2 to 6 J. They also studied the effect of repeated, multiple impacts. They concluded that the design of the patch adopted should have a stiffness as close as possible to that of the parent GFRP. However, such a design may well suffer from an undue weight penalty. Tie et al. [19] investigated the impact behaviour of single-sided, CFRP patch repairs which had been adhesively-bonded to a CFRP parent panel at an impact velocity of 3.25 m.s^{-1} and an impact energy of 13.2 J. They studied the shape of the patch and used patches which had the shapes of a circle, a square, a rhombus, a hexagon and an octagon, all with the same nominal area. They found that the use of the circular-shaped patch gave the best impact performance and thus circular patches will be used in the present work. Furthermore, Hou et al. [20] studied single-sided, CFRP patch repairs adhesively-bonded to a CFRP parent panel using circular-shaped patches, again using an impact velocity of 3.25 m.s^{-1} and an impact energy of 13.2 J. They investigated the effect of varying the impact location from 0 to 50 mm, as the distance from the centre of the repaired parent laminate, i.e. the centre of the circular patch, to the impact point. Their results showed that this distance had little significant effect on the maximum force, or maximum absorbed impact energy, that was recorded. In the present work, the impact point is the centre of the repaired parent laminate, i.e. the centre of the circular patch. Finally, Sun et al. [21] have studied single-sided CFRP patch repairs which were adhesively-bonded to a CFRP parent panel, employing circular-shaped CFRP patches, using impact velocities of 2.82, 3.46 and 4.00 m.s^{-1}, with corresponding impact energies of 10, 15 and 20 J. They conducted three repeated multiple impacts per
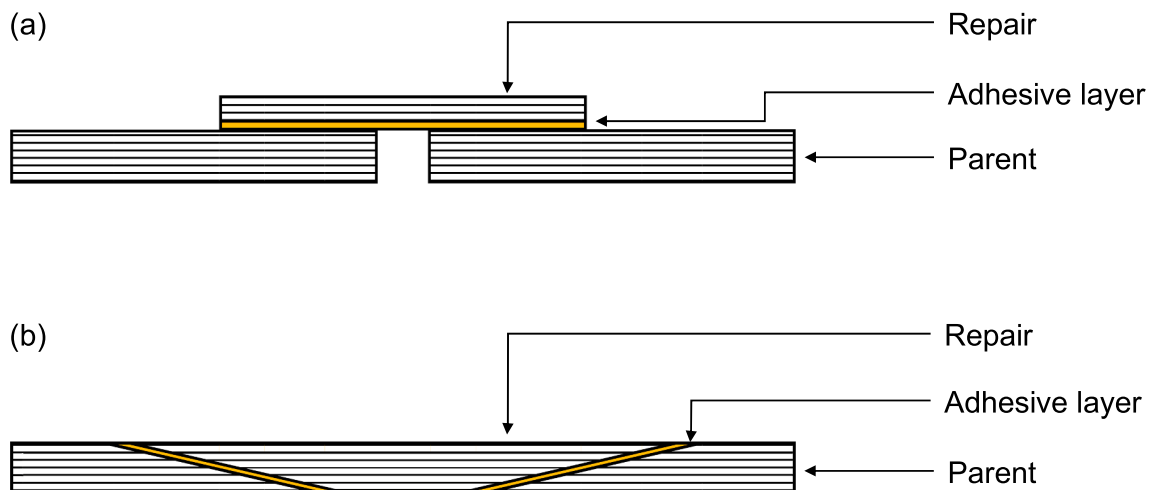

Fig. 1. Schematic of the two main types of repair configurations: (a) patch repair and (b) scarf repair.

test in the centre of the patch and reported that the main damage mechanisms that were observed were intralaminar and interlaminar damage in the CFRP patch-repair. Further, by observing the damage profiles of the panels after repeated impacts, it was found that the damage was mainly interlaminar matrix cracking at an impact energy of 10 J. However, significant fibre fracture occurred in the patch after repeated impacts at impact energies of 15 and 20 J. Further, at an impact energy of 20 J, the patch-repair was actually penetrated and damage to the parent panel was now also observed.

In the present work, single-sided CFRP patch repairs, which are adhesively-bonded to the 'damaged' CFRP parent panel, are subjected to a low-velocity impact with the impact point being the centre of the repaired parent laminate, i.e. the centre of the circular patch. However, in the present work a relatively wide range of impact energies of 7.5, 10.5 and 30 J are employed. The effect of repeated, multiple impacts at these relatively high impact-energies are investigated on the pristine CFRP panel. These tests enable the typical impact-damaged area that results in such panels to be defined. For the repair panels, a hole is cut out in the centre of the parent panel, which represents removal of the impact damage. A single-sided, circular CFRP patch is then bonded over the hole so generated. The effects of the diameter and thickness of the patch are considered, as is the use of a plug of CFRP to fill the hole generated by removal of the 'damaged area' in the composite CFRP parent panel. Load versus time, and load versus displacement, traces are measured from the impact tests on the pristine CFRP panel and the patch-repair CFRP panels, and detailed maps of the interlaminar damage suffered by the various panels are also obtained. These experimental measurements are correlated to the various types of pristine and patch-repair CFRP panels studied. The results reported in the present paper will also form the basis for the verification of a detailed numerical model of the repaired CFRP panels [22].

2. Materials and experimental details

The panels used for the present research were manufactured using quasi-isotropic CFRPs made from unidirectional prepreg (MTC510-UD300-HS-33 %RW) supplied by SHD Composites Ltd, UK. This prepreg contains an epoxy matrix (MTC510) and T700 carbon fibres at a fibre volume fraction of 60%. Flat panels were prepared using an autoclave and cut using a cut-off saw according to
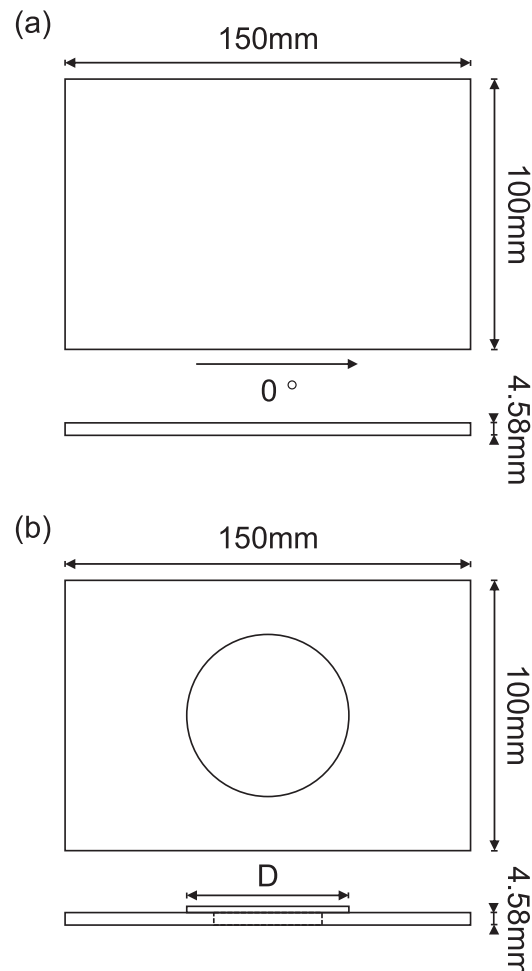

Fig. 2. Plan- and side-views of (a) the pristine panel and (b) the patch-repair CFRP panel.

ASTM D7136 [23]. The prepreg was cured under a constant pressure of 6 bar with a 120 min dwell-time at 110 °C, using a 2 °C per minute temperature ramp. The glass transition temperature of the cured composite was 133 °C. The quasi-isotropic lay-up used for the pristine panels was $[45_2/-45_2/0_2/90_2]_s$, where the 0° plies were aligned with the longer edge of the panels, which had a size of 100 mm × 150 mm, with a thickness, t, of 4.58 mm, as shown in Fig. 2 (a).

The patch-repair panels were produced by removing a 40 mm diameter disk from the centre of a pristine panel, which now became the parent CFRP composite, and a circular patch of quasi-isotropic CFRP material was then adhered over the hole using one layer of MTFA-500 toughened epoxy-film adhesive, supplied by SHD Composites Ltd, UK, which had a nominal thickness of 0.25 mm. The removal of this CFRP disc was performed by Polar Manufacturing Ltd, UK, and consisted of two stages: roughing and finishing. A 2 mm diameter carbide corn-cutter, at a spindle speed of 5000 rpm and feed rate of 300 mm/minute, and a 2 mm diameter carbide 3-flute end mill, at a spindle speed of 5000 rpm and feed rate of 400 mm/minute, were used for the roughing and finishing stages, respectively. Approximately 0.1 to 0.2 mm of CFRP material was left untrimmed after the roughing stage to ensure a high-quality finish. During machining, each pass only removed 1 mm of material in the Z-plane and started and finished away from the hole edge to minimise any damage initiation as far as possible. The machine was run without coolant and the panels were fixed to a sacrificial back-plate with double-sided tape and constrained with clamps. The surfaces of the parent, patch and plug (where relevant) were prepared prior to bonding using 50 grit sanding discs and then cleaned with acetone. The adhesive layer was cured under a constant pressure of 6 bar with a 90 min dwell time at 130 °C and a 3 °C per minute temperature ramp. Two different thicknesses of the patch composite were employed, with the thinner patch having a lay-up of [45/-45/0/90]$_s$ which gave a cured ply thickness, 0.5 t, of 2.29 mm, and the thicker patch having the same lay-up and thickness, t, of 4.58 mm as that of the parent CFRP. Some repairs were made with a push-fit plug of the CFRP parent composite to fill the 40 mm hole, whilst in other repair panels the hole was left unfilled. Where a plug was present, the orientation of the plies was identical to the parent panel and, since a disk of the film adhesive was used, both the parent panel and the plug were adhered to the patch. However, it was found from manufacturing and testing successive batches of patch-repair panels, that a relatively easy push-fit of the composite plug into the 40 mm hole was preferable to a very tight fit. Since the former enabled the adhesive to flow into the gap between the plug and the parent CFRP, and so prevented the patch from being dislodged on a few occasions during impact tests on the repaired panels. Such a failure mode resulted in the repaired panel having a relatively poor impact performance. Therefore, all the current tests using plugs were conducted on patch-repair panels where the composite plug was a relatively easy push-fit into the 40 mm diameter hole which had been cut out in the parent CFRP. This enabled the adhesive to flow into the gap between the plug and the parent CFRP and so prevented the patch from being dislodged during the impact test. Two different diameters of CFRP patches were used: 55 and 65 mm, as denoted by the dimension 'D' in Fig. 2 (b).

The pristine and patch-repair panels were tested under a low-velocity impact loading using an Instron 9340 drop-weight tower supplied by CEAST, Italy, shown in Fig. 3, following the same test method as described elsewhere [10–12]. Basically, the panels were held in place with four rubber clamps, one at each corner, over a fixture with a 125 × 75 mm^2 cut out window. A 16 mm diameter, stainless steel, round-nosed impactor with an overall mass of 5.27 kg was used to impact the panels from varying heights to give impact energies of 7.5, 10.5 or 30 J, with corresponding impact velocities of 1.69, 2.00 and 3.38 m.s^{-1}, respectively. A catching system was
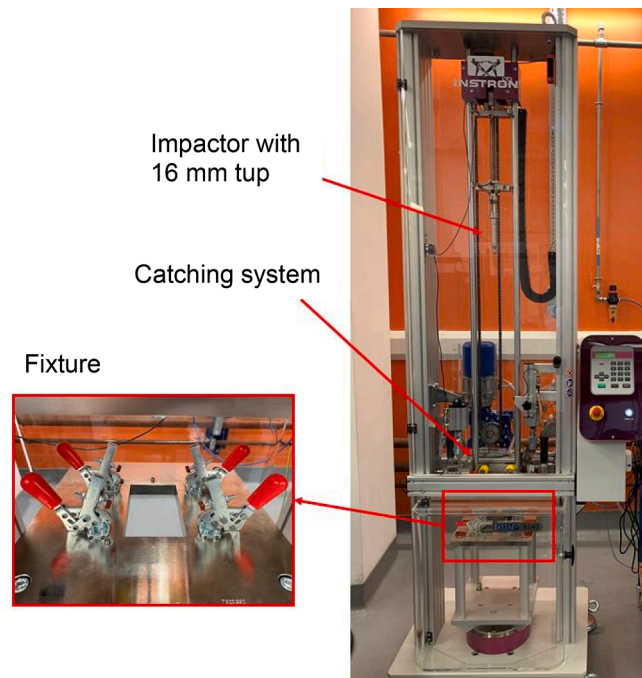

Fig. 3. Drop-weight tower set-up.

used to prevent further impact events from occurring after the initial impact. No software filtering was applied to the load versus time data that was outputted and the accompanying software, provided by CEAST, produced both the impact load and resulting displacement of the panel as a function of time for the impact event. The impacted panels were inspected using a Prisma portable ultrasonic C-scanner supplied by Sonatest Ltd, UK (see Fig. 4) to detect any interlaminar damage area. This technique has been discussed in detail elsewhere [12]. Essentially, a water spray was applied to the surface to act as a contact agent to ensure effective transmission of the ultrasonic waves from the transducer probe through the composite, using a scanning frequency of 5 MHz. These waves are reflected back to the transducer upon interacting with any delamination damage in the panel, and the position and size of the interlaminar damage can be determined from the total travel time and amplitude received by the transducer, respectively. The C-scanning equipment gave images with a scale from 0 to 4.58 mm (i.e. the thickness, t, of the pristine and parent panel, and also of the thicker patch) or 0 to 2.29 mm (i.e. the thickness, 0.5 t, of the thinner patch). The total damage area was then calculated by counting the number of pixels that were not dark blue in colour, since dark blue corresponds to a region of the laminate free from interlaminar damage.

3. Results: Impacting the pristine panels

Repeat, i.e. multiple, impact tests were performed on the pristine CFRP panels, using impact energies of either 7.5, 10.5 or 30 J. Three successive impacts were performed for the highest and lowest impact energies and two were performed for the 10.5 J case. Figs. 5, 6 and 7 show the load against time, and load against displacement, traces for each impact energy value.

From Fig. 5, for an impact energy of 7.5 J, it can be seen that, when subjected to a first impact, there are relatively small amplitude, sinusoidal oscillations on the rising part of the load versus time, and load versus displacement, experimental curves up to a load of 4693 N. These oscillations have been observed previously by other researchers and are indicative of mass-spring oscillations, as first analysed in detail in [12,24–28]. Once a local peak of approximately 4693 N is achieved, at a time of 1 ms, there is an appreciable decrease in the load, and an increase in the associated subsequent oscillations. This significant load drop is indicative of the initiation of damage in the pristine CFRP panel. These oscillations that occur after the first point of this significant load drop, which is often called the initiation load, are typically associated with the first damage of the CFRP panel that occurs, e.g. matrix cracking, indentation including plasticity of matrix and subsequent damage propagation, but does not exclude the formation of delaminations, as has been described in detail by Liu et al. [12] and Bienias et al. [28]. However, both the load traces for the second and third impact events do not show this characteristic, implying that additional damage processes are not initiated but instead existing damage propagates due to the loading by the second or third impact. Furthermore, the peak (i.e. maximum) impact load is noticeably lower for the first impact compared to the second and third impacts. This observation arises because, in the first impact, the impact energy is dissipated through the damage that occurs at the load drops. For the subsequent second and third impacts, the CFRP panel has become softer and the
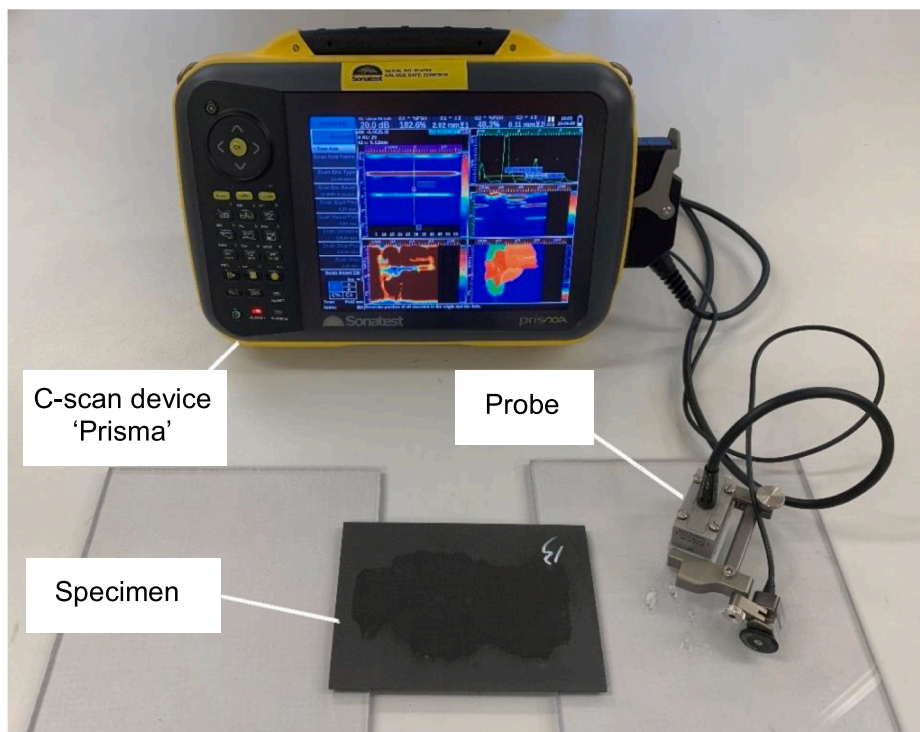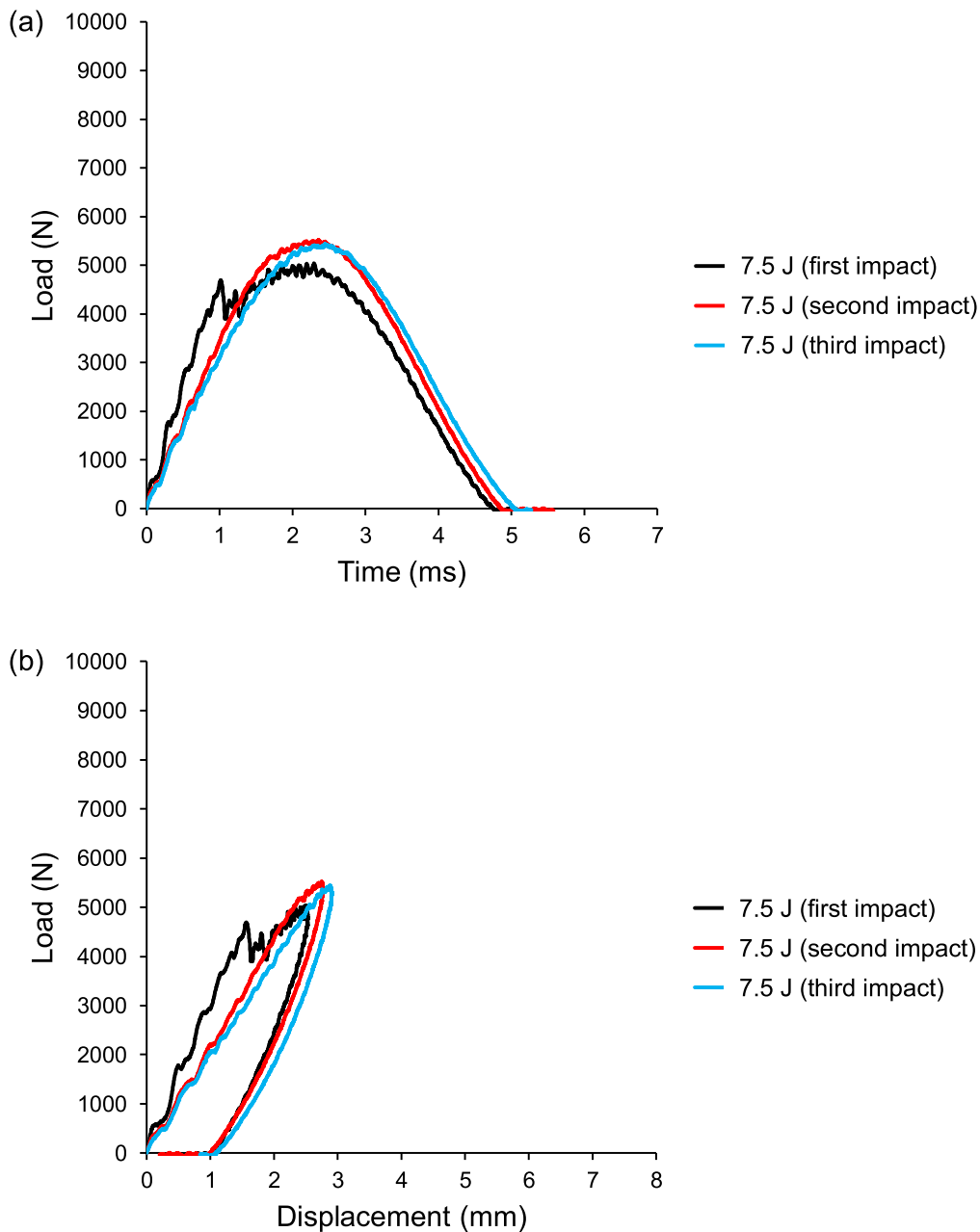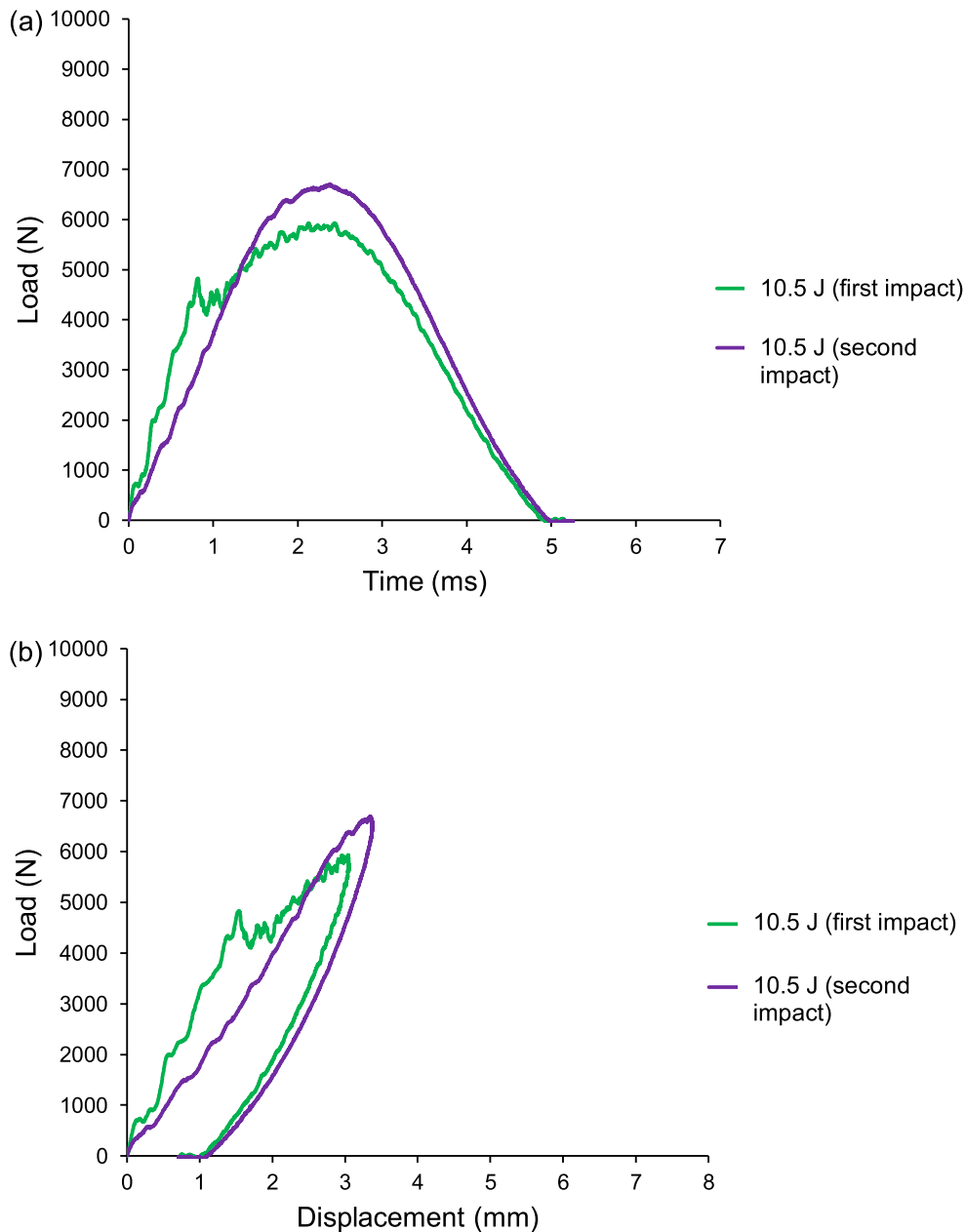

Fig. 4. Ultrasonic C-scan equipment set-up.

Fig. 5. Load traces for repeated, i.e. multiple, impacts on a pristine CFRP panel at 7.5 J: (a) load versus time traces and (b) load versus displacement traces.

effective damage threshold has increased due to the first impact. Thus, more energy can be stored through elastic deformation and a higher load and displacement of the panel are achieved.

Similarly, Fig. 6, for an impact energy of 10.5 J, shows the same trends as for the 7.5 J impact energy tests, and the load traces again exhibit a change in gradient, or load drop, at 4800 N at a slightly reduced time of approximately 0.8 ms. Again, as for the 7.5 J impacts tests, damage is initiated during the first impact but not by the second impact. Both the tests conducted at 7.5 and 10.5 J use a relatively low impact-energy and so a 30 J impact test was next conducted. From Fig. 7, it can be seen that the load traces for the 30 J tests show that the first impact results in a very clear load drop at 5130 N, at an even shorter time of approximately 0.5 ms, followed by significant oscillations, indicative of damage initiation. At this higher impact energy of 30 J, the second and third impacts also exhibit a change in gradient and a load drop with accompanying oscillations, at a load of approximately 9000 N, indicative of further damage initiating. For this increased impact energy of 30 J then after the second and third impacts there also appears to be other damage processes that are initiated besides delaminations, e.g. transverse cracking along the fibres was observed on the rear face of the panels.

Fig. 6. Load traces for repeated, i.e. multiple, impacts on a pristine CFRP panel at 10.5 J: (a) load versus time traces and (b) load versus displacement traces.

The C-scan images shown in Fig. 8 reveal the changes in the area of the interlaminar damage with each successive impact. The right-hand side scale in Fig. 8, and similar figures later, indicates the location of the measured interlaminar delaminations as a function of the depth through the thickness of the panel, where the dark-red colour represents a reflection from the surface nearest the transducer probe and the dark-blue colour represents a reflection from the surface furthest away from the transducer probe, i.e. often the rear (non-impacted) surface. The delaminations form between plies of different fibre orientations and the colour code indicates their distance from the transducer probe. Each delamination tends to grow along the orientation of the ply beneath the delamination on the lower surface. The results show, for example, that the damage area footprint, which encompasses all delaminations, appears to grow by ca. 50% following the second impact for all the three energy levels studied. For the third impact at 7.5 J, the increase in the damage area is reduced to ca. 25%. Whilst, for the 30 J impact, the damage area has almost reached a maximum after the second impact and there is only a very slight further increase of ca. 5% for the third impact. From these impact tests on the pristine CFRP panel it was decided to cut out a 40 mm diameter hole in the centre of the parent CFRP panel, since this is a good representation of the typical extent of impact damage in the CFRP corresponding to an impact energy of 7.5 J. Also, the presence of such a hole, i.e. 'damage area', gives a
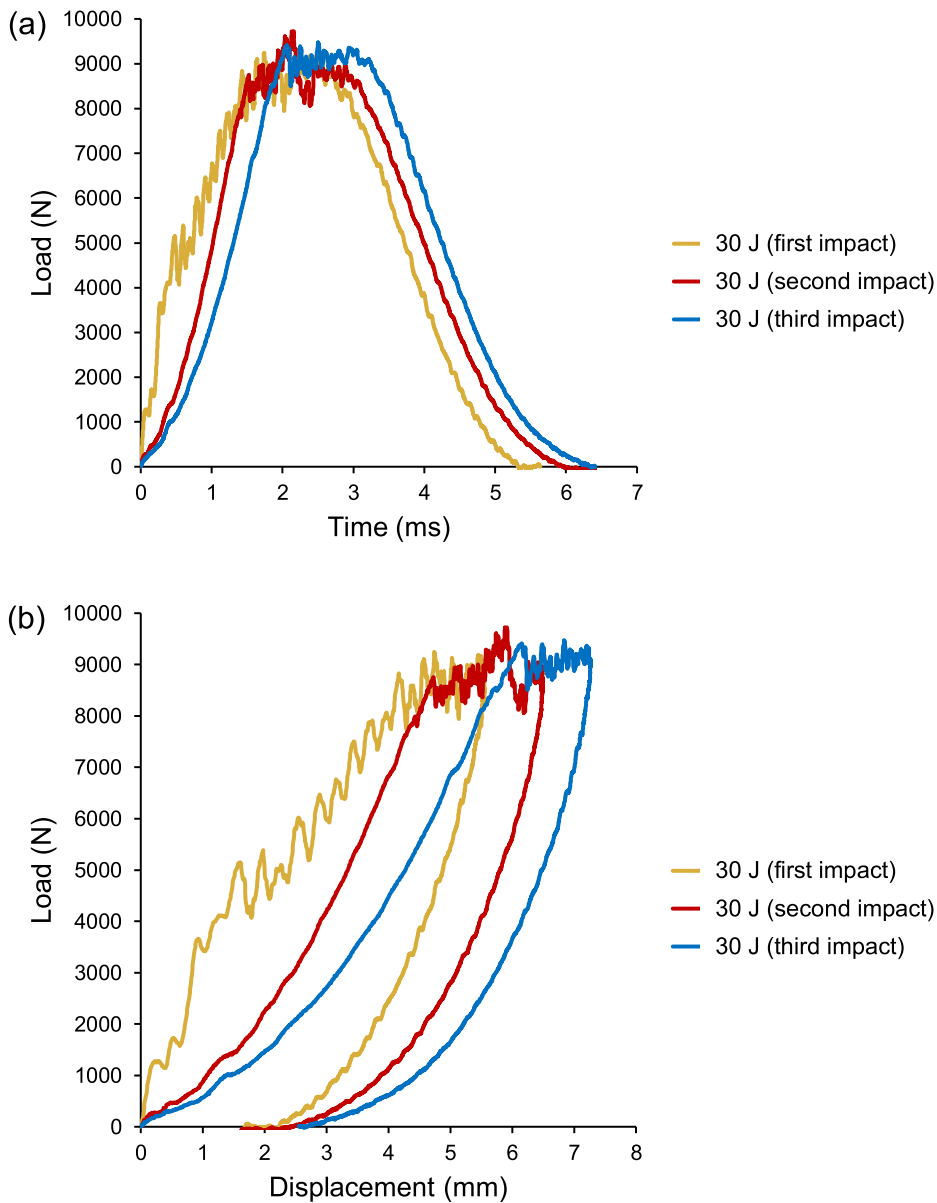
Fig. 7. Load traces for repeated, i.e. multiple, impacts on a pristine CFRP panel at 30 J: (a) load versus time traces and (b) load versus displacement traces.

significant change in the measured impact response of the panel at 7.5 J but is not so large in size that edge-effects will be observed when the patch-repair CFRP panels are impacted.

4. Results: Impacting the Patch-Repair panels

4.1. Effect of varying the patch diameter, with a plug present

Four repair panels with CFRP plugs were manufactured in total: two for each patch diameter, i.e. 55 mm and 65 mm, with a patch thickness, 0.5 t, of 2.29 mm. For these patch-repair panels with a plug present, the load versus time, and load versus displacement traces are compared to the performance of the pristine CFRP panel in Fig. 9 for an impact energy of 7.5 J. From these traces, it can be seen that the overall stiffness of the panel and the initial damage load are increased, and the maximum displacement is reduced, when a repair is undertaken using a plug. This is mainly due to the increase in the overall thickness that the patch and plug together add to the patch-repaired CFRP parent panel, compared to that of the pristine CFRP panel. However, there is a more sudden drop in the load after damage initiation in the repaired panel compared to the pristine panel, which could be due to the overall increased stiffness of the
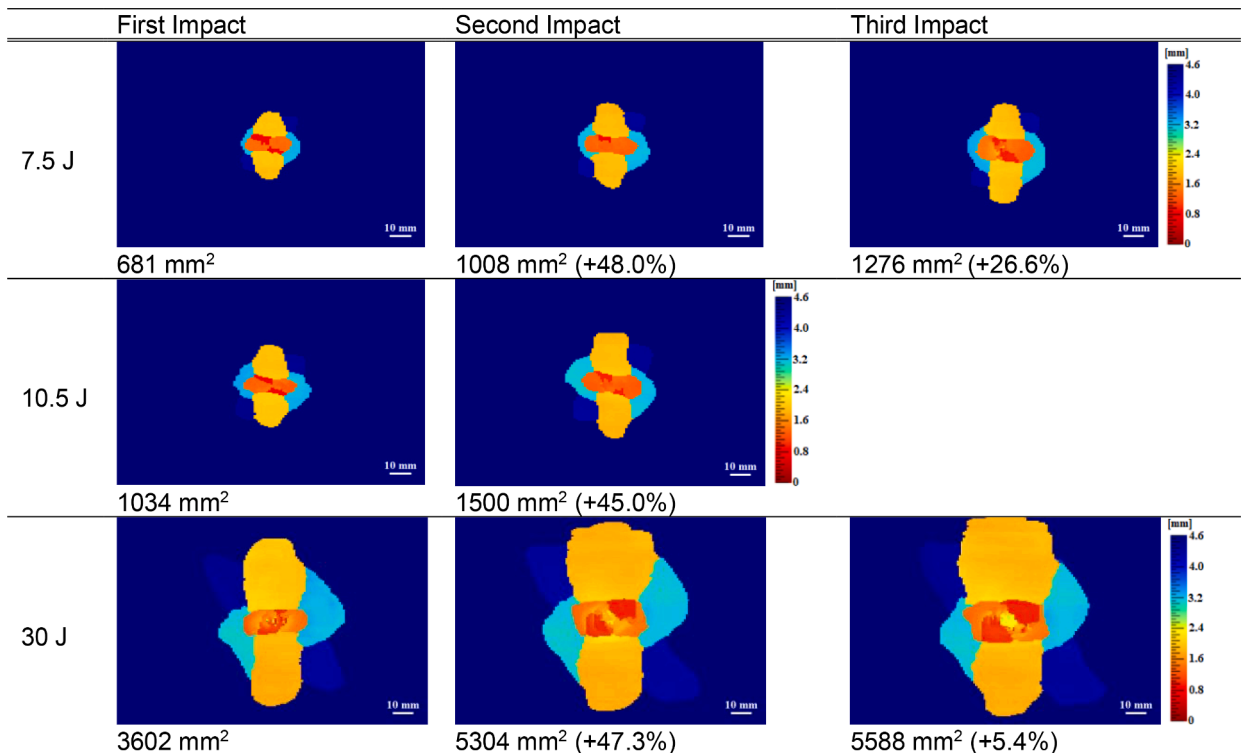
Fig. 8. C-scan images taken from the top (impacted) surface for repeated, i.e. multiple, impacts on pristine CFRP panels at various impact energies. (The scales show the depth of the different locations of the interlaminar damage. The percentage value, in brackets, is relative to the preceding impact.).

panel but which could also arise from damage around the plug.

A notable point about Fig. 9 is that the load versus time, and load versus displacement, traces for the patch-repair panels with a plug have a higher maximum load of just under 7880 N, at a time of approximately 1.2 ms, for the 65 mm diameter patch and 7550 N, at a time of approximately 1.2 ms, for the 55 mm diameter patch, compared to the pristine CFRP panel. In both cases, there is a significant load drop, indicative of damage initiation. Thus, an increase in patch diameter to 65 mm is somewhat beneficial in raising this initiation load from 7550 to 7880 N, as would be expected. Furthermore, these initiation loads are indeed much higher than for a pristine panel, i.e. 4693 N at 1 ms. For all these patch-repair panels with a plug, as for the pristine panel on first impact, there are slight oscillations in the load up to the maximum value due to mass-spring oscillations. Clearly, adding a patch of thickness, 0.5 t, of 2.29 mm, together with a CFRP plug, of thickness, t, of 4.58 mm, is very beneficial in restoring the overall structural response of the parent CFRP composite, of thickness, t, of 4.58 mm, and this is evident by the increase in the initiation load and the stiffness for the patch-repair CFRP panels with a plug.

Fig. 10 shows the C-scan images of the interlaminar damage area in the 55 and 65 mm diameter patch-repair CFRP panels containing a plug, compared to that of a pristine CFRP panel. All were impacted at the same impact energy of 7.5 J. It is clear that the damage area is greatly reduced when the repairs have been performed. If no repair had been performed after a 7.5 J impact and the panel was hit for a second time, the damage in the panel in Fig. 10 (a) would have increased even further, by ca. 50% given the results discussed above. This again demonstrates the effectiveness of patch repairs when a plug is also employed at preventing further damage and restoring the impact properties even beyond that of the pristine CFRP panel. Additionally, a C-scan from the rear-face of the repair panels was performed to allow the damage in the plug to be observed and such scans also confirmed that there was no delamination damage in the parent material. Fig. 11 shows these scans, with the damage area in the plug being larger than that in the patch, but still less than that in the pristine panel after just one impact. This further demonstrates the success of a patch repair with a plug in restoring the impact properties of a damaged panel.

### 4.2. Effect of varying the patch diameter, with no plug present

To consider the effect of having no plug in the repair, panels were manufactured with patch repairs but with no plug present and impacted at 7.5 J, and two different diameters of patch of 55 and 65 mm were used. As before, the patch thickness, 0.5 t, was 2.29 mm and the thickness, t, of the parent composite was 4.58 mm. Fig. 12 shows the load versus time, and load versus displacement, traces for the two types of patch-repair panels, compared to a pristine panel. It can be seen that the loading response for both diameters of patch are similar but quite different to that of a pristine panel. For the smaller diameter patch (i.e. 55 mm diameter, with 0.5 t of 2.29 mm),
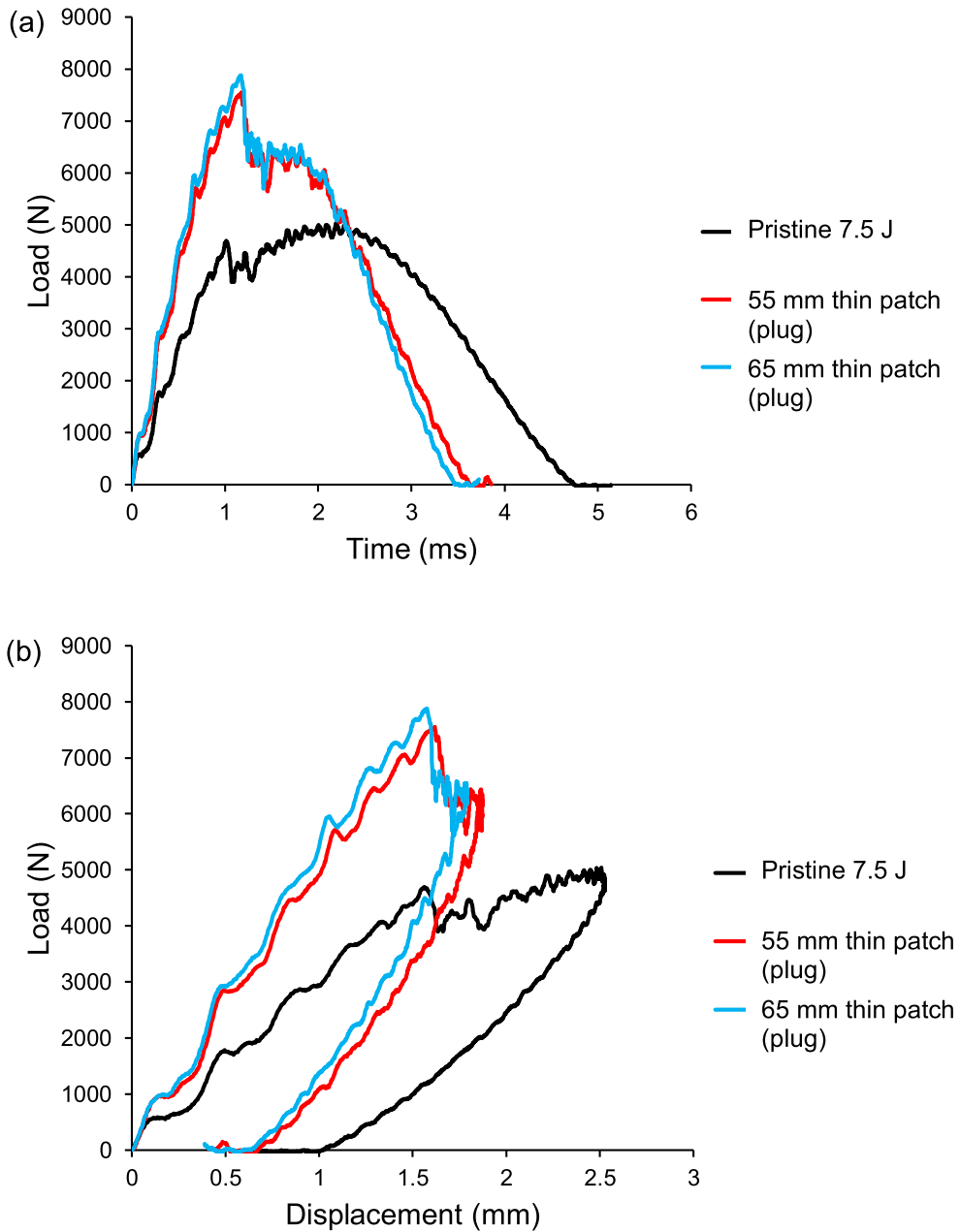
Fig. 9. Load traces for a pristine CFRP panel and 55 mm diameter and 65 mm patch-repair panels, with a CFRP plug, impacted at 7.5 J. The thickness, t, of the parent and the plug CFRP was 4.58 mm and the thickness, 0.5 t, of the patch was 2.29 mm. Shown are the: (a) load versus time traces and (b) load versus displacement traces.

the initiation load is 1771 N at a time of approximately 0.6 ms. Whilst for the larger diameter patch (i.e. 65 mm diameter, with 0.5 t of 2.29 mm), the initiation load is 1689 N at a time of approximately 0.6 ms. For comparison, the initiation load for a pristine sample is 4693 N at a time of approximately 1 ms.

Therefore, for both patch diameters, the thinner patch, when it is not supported by a plug, deforms more easily around the drop-weight impact site where the impact stress is initially localised and concentrated. Thus, the accompanying localised strain gradients will initiate damage more readily at a lower initiation load. In both cases, as is evident in Fig. 13, there is appreciably more inter-laminar damage in the patch with no plug present, i.e. 1365 mm^2 for a patch diameter of 55 mm and 1252 mm^2 for a patch diameter of 65 mm, compared to that in (a) the pristine panel, i.e. 681 mm^2, and (b) the patch-repairs containing a plug, see Fig. 10. For the patch repairs containing no plug, Fig. 13 shows that the delaminations in the patch extend to, and overlap very slightly, the edge of the hole in the parent CFRP, as defined by the white-dashed line. The parent CFRP surrounding this white-dashed line supports the patch repair
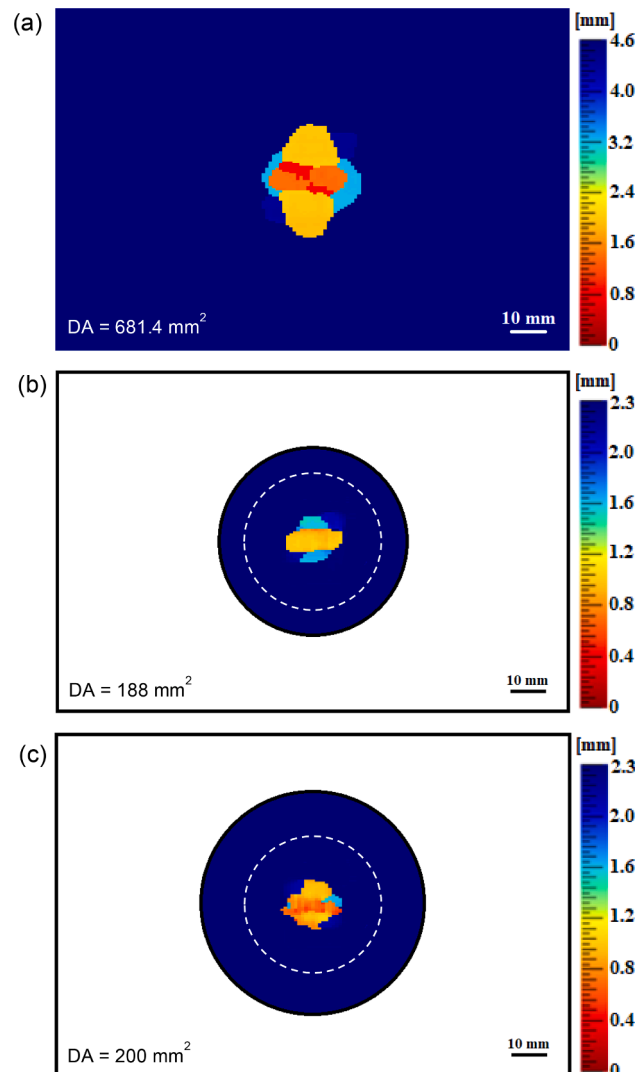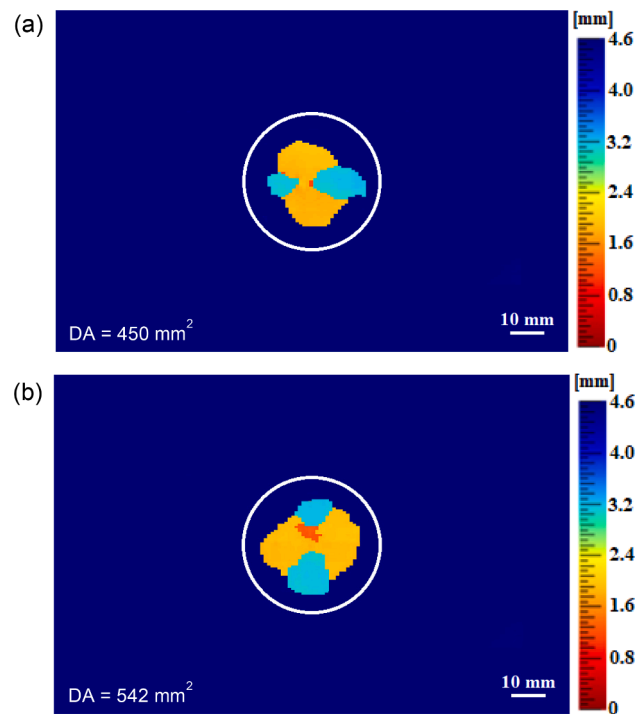
Fig. 10. C-scan images taken from the top (impacted) face after a 7.5 J impact for: (a) the pristine CFRP panel (of thickness, t, of 4.58 mm), (b) the 55 mm patch-repair CFRP panel (of patch thickness, 0.5 t, of 2.29 mm, with a plug) and (c) the 65 mm patch-repair CFRP panel (of patch thickness, 0.5 t, 2.29 mm, with a plug). The plug was 4.58 mm thick, i.e. the same thickness as the parent CFRP. (The white-dashed line represents the 40 mm diameter hole that was initially cut out in the parent panel.).

and inhibits further delaminations. C-scans were also taken from the rear face of the repair panels on the parent CFRP and, again, these tests revealed that there was no delamination damage in the parent CFRP composites.

4.3. Effect of varying the patch thickness, with no plug present

Another variable for the repair patch was the patch thickness. Two different thicknesses were studied with no plug present and the thicknesses, 0.5 t and t, used were 2.29 and 4.58 mm, with the parent composite always having a thickness, t, of 4.58 mm. The patch diameter chosen for this study was 65 mm and neither of the repaired panels had a plug inserted into the machined hole. The panels were impacted at an energy of 7.5 J.

Fig. 14 shows the load versus time, and load versus displacement, traces for both the thicker patch (thickness, t, of 4.58 mm) and the thinner patch (thickness, 0.5 t, of 2.29 mm) repair panels, all with a patch diameter of 65 mm and with no plug present, compared to a pristine panel. It can be seen that, with a thick patch and no plug, the loading response is very similar to that of the pristine CFRP panel. In contrast, the thinner patch results in a lower stiffness and a peak (i.e. maximum) load of around 1000 N less than both the pristine and thick patch-repair panels. For the thick patch, i.e. t = 4.58 mm, the initiation load is 5249 N at a time of approximately 0.7 ms and for a thin patch, i.e. 0.5 t = 2.29 mm, the initiation load is 1689 N at a time of approximately 0.6 ms. For comparison, the initiation load for a pristine sample is 4693 N at a time of 1 ms. In these patch-repair panels, the thin patch, when it is not supported by a plug, deforms

Fig. 11. C-scan images of the plug and surrounding parent composite taken from the rear (non-impacted) face of the panel after a 7.5 J impact of: (a) the 55 mm patch-repair panel (of thickness, 0.5 t, of 2.29 mm, with a plug) and (b) the 65 mm patch-repair panel (of thickness, 0.5 t, of 2.29 mm with with a plug). The plug was 4.58 mm thick, i.e. the same thickness as the parent CFRP. (The solid-white line is 40 mm in diameter and represents the boundary between plug and the parent CFRP panel.).

more easily and the localised strain gradients will initiate damage more readily at a lower initiation load. The thick patch adds additional material to the parent panel and, in so doing, increases the stiffness and raises the corresponding initiation load. This is clearly very beneficial when no plug is present. The thick patch-repair panel suffers the largest drop in the load after damage initiation, which is possibly due to its relatively higher stiffness. On the other hand, the repair panel using the thinner patch does not exhibit any significant load drops, although there is a slight change in the gradient of the load versus time, and load versus displacement, traces which are indicative of damage initiation at 1689 N. This lower damage initiation load for the panel repaired using the thinner patch is most likely due to the reduction in stiffness from having a thinner patch and no plug present.

The C-scan images from these tests are shown in Fig. 15, with the damage area in all four panels extending up to, and overlapping very slightly, the edge of the 40 mm diameter hole in the parent CFRP beneath the patch, which of course contains no plug in these panels. These images demonstrate that, although both the thin and thick patches have damage areas that exceed what was recorded in the pristine panels, the thicker patch gives an area of around 300 mm^2 smaller than the thinner patch. This implies that doubling the patch thickness improves the repair performance due to an increase in the stiffness of the repaired panel. C-scan images were also taken for the entire thickness, i.e. for the patch and parent panel together, as well as from the rear face, to see if damage was present within the parent laminate or solely the patch. From these C-scan tests, yet again, no damage could be seen in the parent CFRP at all in the patch-repair panels, and so it was concluded that the damage was confined to the patch alone.

4.4. Comparing patch repairs with and without a plug present

The final study in this paper is to compare firstly the addition of a plug in the patch-repair panels versus the patch-repair panels without a plug, using the pristine panel as a baseline. All tests were conducted at an impact energy of 7.5 J. For this study, patches, with diameters of 55 and 65 mm, of half the thickness, 0.5 t, of 2.29 mm of the parent material were used. The load versus time, and load versus displacement, traces are shown in Fig. 16. These results reveal that the presence of a plug increases the stiffness and hence the load before damage initiation of the repaired panel occurs. On the other hand, thin patch-repairs of 0.5 t = 2.29 mm, for both the 55 and 65 mm diameter patches, with no plug present, result in the lowest, and least well defined, load drops at the initiation of damage in the repaired panels, i.e. of 1771 N and 1689 N, respectively. Further, a thin patch-repair (of thickness, 0.5 t, = 2.29 mm) panel, for both 55 and 65 mm diameter patches, with a plug present, results in the highest values of the peak loads of 7550 N (for the 55 mm patch) and 7880 N (for the 65 mm patch), and these designs of repair clearly provide very impact-resistant repaired panels. Secondly, a 65 mm diameter patch of thickness, t = 4.58 mm, with no plug present, results in a load drop which is well defined at 5249 N. The behaviour here is similar to that of the pristine panel with a load drop at 4693 N.
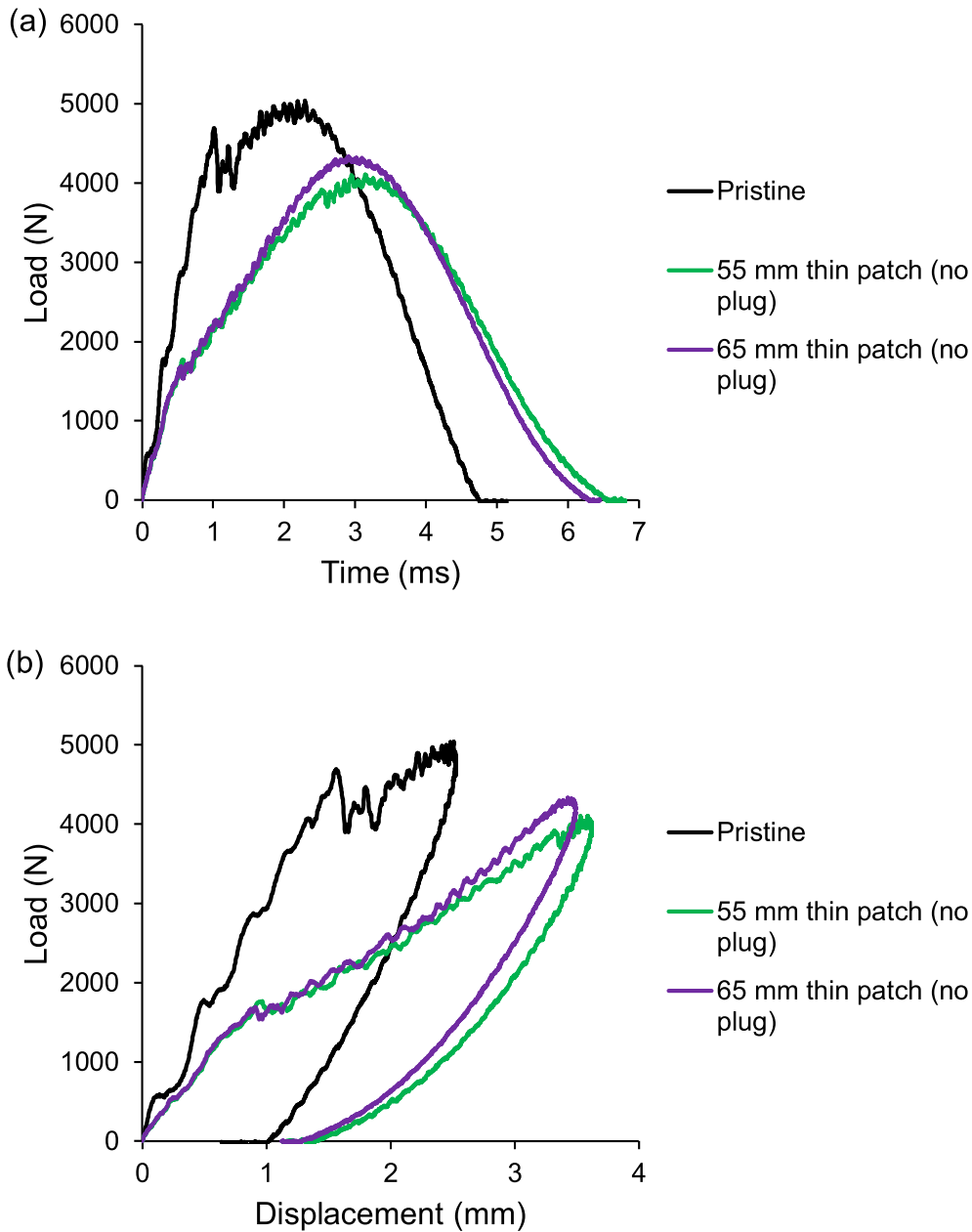
Fig. 12. Load traces for a pristine CFRP panel and 55 mm diameter and a 65 mm patch-repair panels, with no CFRP plug, impacted at 7.5 J. The thickness of the parent was 4.58 mm and the thickness of the patch was 2.29 mm. Shown are the: (a) load versus time traces and (b) load versus displacement traces.

Fig. 17 shows the C-scan images taken of the four panels, as viewed from the top face of the panels. For both the 55 mm and 65 mm diameter patches, with no plug present, the damage area increases over six-fold compared to similar patch repairs but with a plug present. This again demonstrates that the presence of the plug is very beneficial to the impact performance of the repaired panel for both diameters of patch.

5. Discussion

The repair results are summarised in Table 1, which gives the initiation load and time, peak (i.e. maximum) load, maximum displacement and damage area for all the pristine and patch-repair CFRP panels tested under a single impact at an energy of 7.5 J.

Patch-repair panels without a plug were manufactured and tested using duplicate specimens, employing an impact energy of 7.5 J, and the results from these duplicate patch-repair panels are shown in Table 1. There are several noteworthy points. Firstly, all the
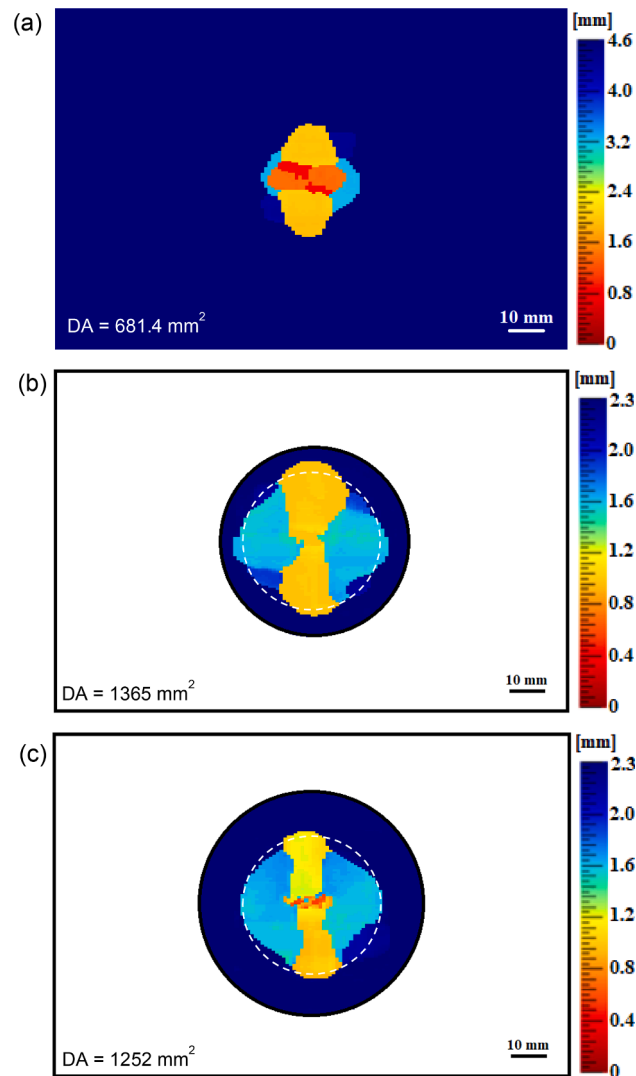
Fig. 13. C-scan images taken from the top (impacted) face after a 7.5 J impact for: (a) the pristine CFRP panel (of thickness, t, of 4.58 mm), (b) the 55 mm patch-repair panel (of patch thickness, 0.5 t, of 2.29 mm, with no plug) and (c) the 65 mm patch-repair CFRP panel (of patch thickness, 0.5 t, 2.29 mm, with no plug). The thickness, t. of the parent CFRP was 4.58 mm. (The white-dashed line represents the 40 mm diameter hole that was initially cut out in the parent panel.).

measured impact properties are seen to be in good agreement from the two tests, i.e. for Test 1 versus Test 2, for each type of repair with no plug present. To further illustrate this point, the variation in the damage area was calculated between each pair of panels. The percentage variation in the values of the measured damage area is found to be ± 6.8%, ±0.8% and ± 2.4% for the 55 mm thin patch, 65 mm thin patch and 65 mm thick patch-repair panels respectively, see Table 1. The very good agreement in the measured impact load traces, and the low degree of variation in the comparative values of the damage area, reveals a very good repeatability for the manufacture and testing of these patch-repair panels. Secondly, it can be seen that the panels with either plugs, or a thick patch, have relatively high values of the peak load and a lower maximum displacement than the pristine panel. However, the patch-repair panels manufactured using a plug are the only ones that produce a damage area that is significantly smaller than that of the pristine panel. Thirdly, the patch diameter does not seem to significantly affect the impact performance of repaired composites, at least for 55 mm patches compared to 65 mm patches. Fourthly, on the other hand, the patch thickness has a significant effect on the impact perfor-mance of the patch-repair composites. Both the thick patch-repair panel, with no plug, and the pristine panel had peak (i.e. maximum) load values of around 5000 N, compared with the thinner patch, with no plug, that had a peak load value of approximately 1000 N lower. This indicates that the thick patch results, in terms of impact properties, are very similar to those of the pristine panel. Furthermore, the average damage area between two panels with the thinner patch was 296 mm² larger than the average of the two thicker patch-repair panels, demonstrating the superior impact properties of a repair with the thicker patch. Since only half-thickness and full-thickness patches were considered in this research, it is unclear whether the optimum patch thickness is the same thickness as
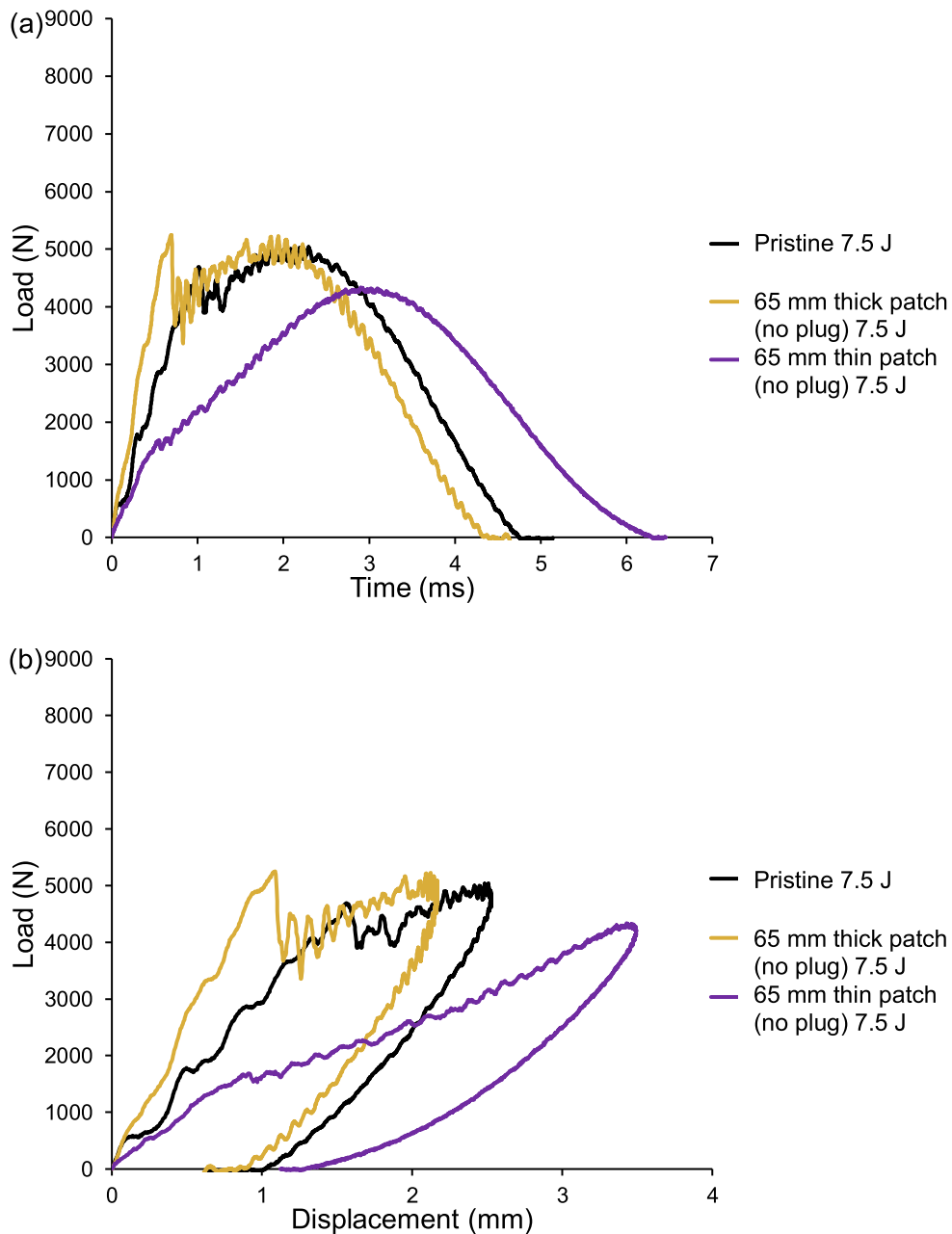
Fig. 14. Load traces for a pristine panel, a 65 mm patch-repair CFRP panel (of patch thickness, t, of 4.58 mm, with no plug) and a 65 mm patch-repair CFRP panel (of patch thickness, 0.5 t, of 2.29 mm, with no plug). Both patch-repair panels were impacted at 7.5 J. Shown are the: (a) load versus time traces and (b) load versus displacement traces.

the original parent CFRP, or whether it would fall somewhere between these two values. Finally, the inclusion of a CFRP plug, to fill the hole created by the removal of the damaged material in the parent CFRP, (a) resulted in a reduction in the damage area of over 1000 mm^2 in the patch, (b) increased the maximum load by around 3500 N and (c) almost halved the maximum displacement. These results therefore show that both the patch thickness and the addition of a plug are repair design features that significantly influence the impact performance of the repaired panel, with the latter feature having the largest effect of all three design variables that were considered.

Thus, when considering the peak load, the maximum displacement and the damage area, the panels repaired with the presence of a plug exhibited an impact performance significantly better than that of the pristine panel, implying that using a thin patch and a plug is the most effective patch repair technique investigated in this paper. An alternative would be to use a thicker patch without a plug, as this gives load traces similar to that of the pristine panel and results in peak load and maximum displacement values greater than those of the pristine panel. A further benefit to this alternative technique is that the initial damage does not have to be cut out before the
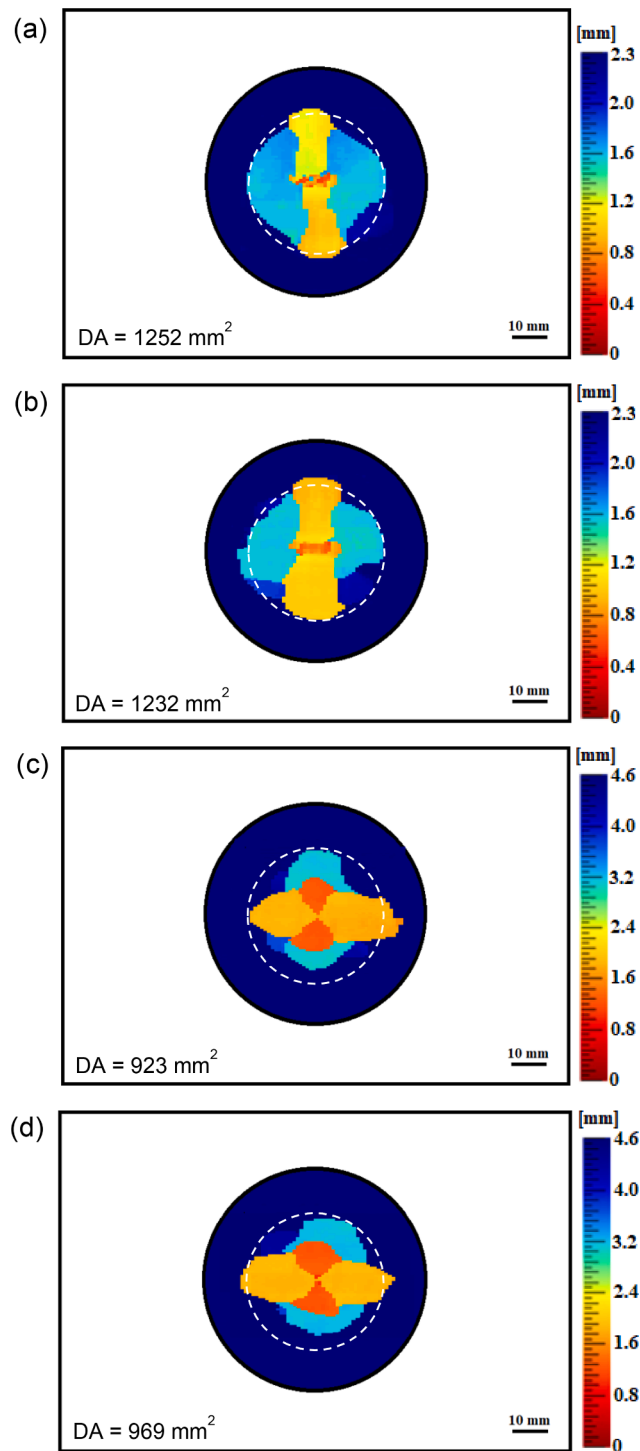
Fig. 15. C-scan images of patch-repair CFRP panels with no plugs taken from the top (impacted) face after a 7.5 J impact for: (a) the 65 mm thin (0.5 t = 2.29 mm) patch repair – Test 1, (b) the 65 mm thin (0.5 t = 2.29 mm) patch repair – Test 2, (c) the 65 mm thick (t = 4.58 mm) patch repair – Test 1, and (d) the 65 mm thick (t = 4.58 mm) patch repair – Test 2. (Tests 1 and 2 are duplicate tests. The white-dashed line represents the 40 mm diameter hole that was initially cut out in the parent panel.).

repair is undertaken, thereby reducing the repair time and the risk of inducing further damage during machining. However, when superior impact properties are required, such as for a critical component, the removal of the initial damage and the inclusion of a plug would be beneficial, since this design of repair was found to restore the impact performance to that of a pristine panel. Additionally, it
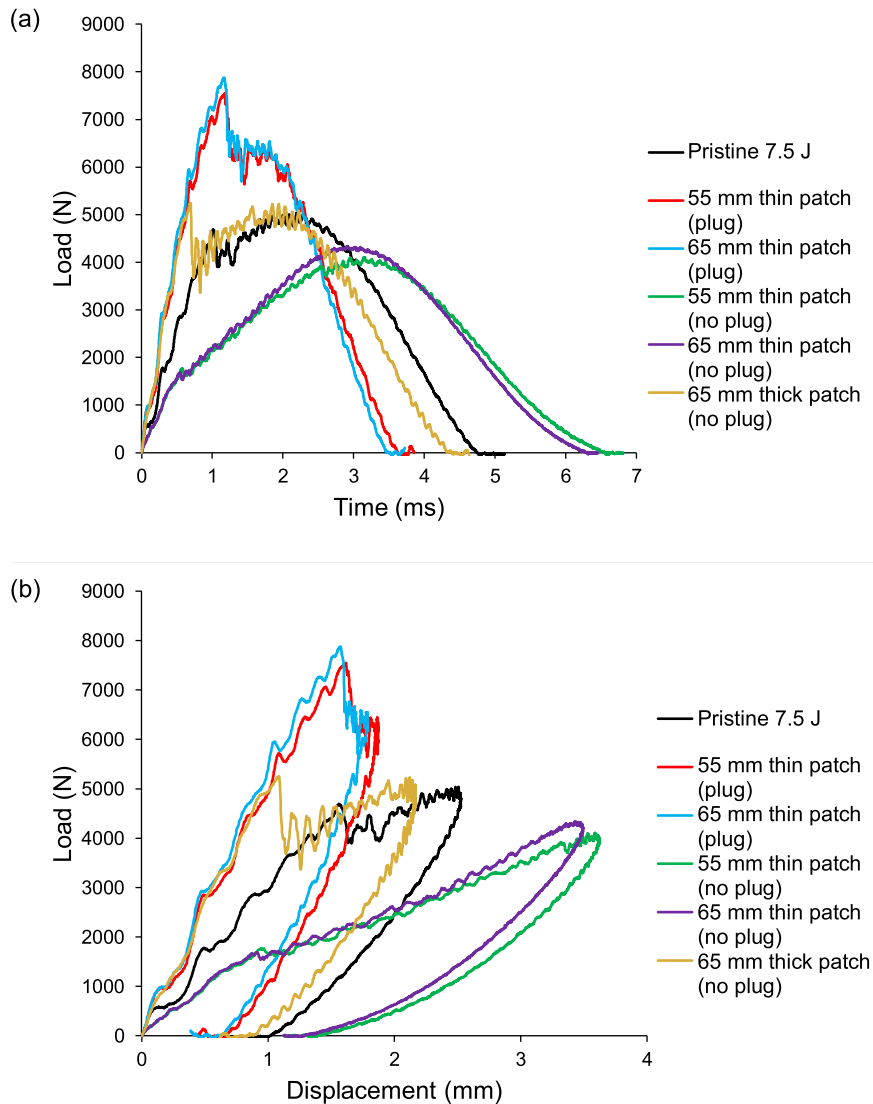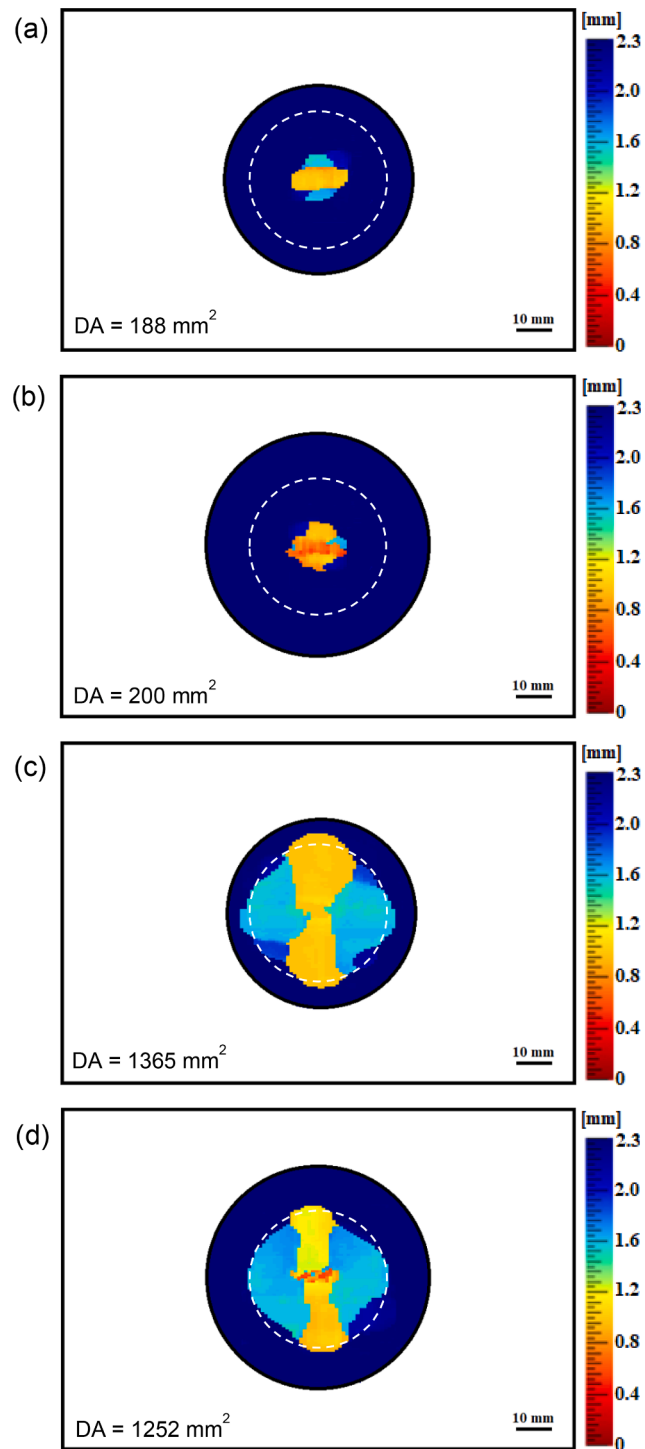
Fig. 16. Load traces for the pristine panel, the 55 mm diameter thin (0.5 t = 2.29 mm) patch-repair panel with a plug, the 65 mm diameter thin (0.5 t = 2.29 mm) patch-repair panel with a plug, the 55 mm thin (t = 2.29 mm) patch-repair panel with no plug, the 65 mm thin (0.5 t = 2.29 mm) patch-repair panel with no plug and the 65 mm thick (t = 4.58 mm) patch-repair panel with no plug. All impacted at 7.5 J: (a) load versus time traces and (b) load versus displacement traces.

should be noted the use of a relatively thicker patch would likely result in inferior aerodynamic performance, thus making a thin patch with the inclusion of a plug a potentially more suitable repair technique.

6. Conclusions

In conclusion, impact testing on pristine CFRP and CFRP patch-repair panels has been performed to investigate the suitability of a single-sided, adhesively-bonded CFRP patch to restore the impact properties of damaged CFRP panels. The primary findings were:

- Interlaminar damage observed from the ultrasonic C-scans is clearly linked to a marked initiation load drop in the load versus time and load versus displacement traces. The delaminations form between plies of different fibre orientations and tend to grow along the orientation of the ply beneath the delamination.
- Repeat impacts on pristine panels at 7.5, 10.5 and 30 J demonstrated that the damage area increases by almost 50% when impacted for a second time. Impacting for a third time at 30 J implied an upper-damage threshold that the panel can sustain, with only a small (i.e. 5.4%) incremental increase in the damage area in comparison to the second impact at 7.5 J.

Fig. 17. C-scan images of patch-repair CFRP panels taken from the top (impacted) face after 7.5 J impact for: (a) the 55 mm diameter thin (0.5 t = 2.29 mm) patch-repair CFRP panel with a plug present, (b) the 65 mm diameter thin (0.5 t = 2.29 mm) patch-repair CFRP panel with a plug present, (c) the 55 mm diameter thin (0.5 t = 2.29 mm) patch-repair CFRP panel with no plug present and (d) the 65 mm diameter thin (0.5 t = 2.29 mm) patch-repair CFRP panel with no plug present. (The white-dashed line represents the 40 mm diameter hole that was initially cut out in the parent panel.).

Table 1
Measured impact behaviour of the pristine and patch-repair CFRP panels, with all panels impacted at 7.5 J.

Panel and test number	Drop-weight traces					Damage area (mm^2)		Variation in damage area
		Damage initiation load (N)	Damage initiation time (ms)	Peak load (N)	Max. displacement (mm)	Patch	Plug	
Pristine (first impact)		4693	1.0	5040	2.4	681		–
Diameter 55 mm Patch (with plug) Thin (2.29 mm)		7550	1.2	7550	1.8	188	450	–
Diameter 65 mm Patch (with plug) Thin (2.29 mm)		7880	1.2	7880	1.7	200	542	–
Diameter 55 mm Patch (no plug) Thin (2.29 mm)	1	1771	0.6	4106	3.4	1365	–	±6.8%
	2	1785	0.6	4078	3.4	1191	–	
Diameter 65 mm Patch (no plug) Thin (2.29 mm)	1	1689	0.6	4335	3.3	1252	–	±0.8%
	2	1717	0.6	4200	3.4	1232	–	
Diameter 65 mm Patch (no plug) Thick (4.58 mm)	1	5249	0.7	5249	2.1	923	–	±2.4%
	2	5362	0.7	5362	2.1	969	–	

- Using a patch-repair of half the thickness of the parent panel, with no plug, produced delamination damage greater in extent than the pristine panel incurred, but it was all contained within the patch and did not spread into the parent panel. These observations arise since the thin patch, when it is not supported by a plug, deforms relatively easily and the localised strain gradients that result initiate damage more readily at a lower initiation load.

- Using a thicker patch of the same thickness as the parent material, but with no plug, resulted in a lower extent of delamination damage, at 7.5 J, but this was still more than that observed for the pristine panel for the same impact energy. Again, the delamination damage was contained within the patch and thus protected the surrounding parent material.

- Using a patch of half the thickness of the parent panel, together with a plug of identical thickness and lay-up to the parent panel, resulted in impact properties superior to that of the pristine CFRP panel, suggesting that this is a very good patch-repair configuration. Indeed, the delamination area in the patch was found to be less than that seen in the pristine panel for the same impact energy.

- For a given design, there were found to be no clear, major overall benefits to be gained by increasing the patch diameter from 55 mm to 65 mm.

- To summarise, patch-repair panels with either a plug, or having a relatively thick patch, give higher values of peak load and a lower maximum displacement than that recorded for the pristine panel upon testing at a given impact energy. However, the patch-repair panels manufactured using a plug are the only designs that produce a resulting interlaminar damage area that is smaller than that seen in the pristine panels, tested at the same impact energy. Thus, adding a CFRP plug when undertaking a patch-repair clearly increases the structural performance of the repaired CFRP panel.

Declaration of Competing Interest

The authors declare that they have no known competing financial interests or personal relationships that could have appeared to influence the work reported in this paper.

References

[1] Cantwell WJ, Morton J. Detection of impact damage in CFRP laminates. Compos Struct 1985;3:241–57. https://doi.org/10.1016/0263-8223(85)90056-X.

[2] Dorey G, Bishop SM, Curtis PT. On the impact performance of carbon fibre laminates with epoxy and PEEK matrices. Compos Sci Tech 1985;23:221–37. https://doi.org/10.1016/0266-3538(85)90019-3.

[3] Cantwell WJ, Morton J. Comparison of the low and high velocity impact response of CFRP. Compos 1989;20:545–51. https://doi.org/10.1016/0010-4361(89)90913-0.

[4] Cantwell WJ, Morton J. The influence of varying projectile mass on the impact response of CFRP. Compos Struct 1989;13:101–14. https://doi.org/10.1016/0263-8223(89)90048-2.

[5] Ghaseminejhad MN, Parvizi-Majidi A. Impact behaviour and damage tolerance of woven carbon fibre-reinforced thermoplastic composites. Constr Build Mater 1990;4(4):194–207.

[6] Cantwell WJ, Morton J. The impact resistance of composite materials - a review. Compos 1991;22:347–62. https://doi.org/10.1016/0010-4361(91)90549-V.

[7] Morita H, Adachi T, Tatesiha Y, Matsumoto H. Characterization of impact damage resistance of CF/PEEK and CF/Toughened epoxy laminates under low and high velocity tests. J Reinf Plastics Compos 1997;16:131–43. https://doi.org/10.1177/073168449701600203.

[8] Batra RC, Gopinath G, Zheng JQ. Damage and failure in low energy impact of fiber-reinforced polymeric composite laminates. Compos Struct 2012;94:540–7. https://doi.org/10.1016/j.compstruct.2011.08.015.

[9] Liu H, Falzon BG, Tan W. Experimental and numerical studies on the impact response of damage-tolerant hybrid unidirectional/woven carbon-fibre reinforced composite laminates. Compos Part B Eng 2018;136:101–18. https://doi.org/10.1016/j.compositesb.2017.10.016.

[10] Liu H, Liu J, Ding Y, Zheng J, Kong X, Zhou J, et al. The behaviour of thermoplastic and thermoset carbon-fibre composites subjected to low-velocity and high-velocity impact. J Mater Sci 2020;55:15751–68. https://doi.org/10.1007/s10853-020-05133-0.

[11] Liu H, Liu J, Ding Y, Zhou J, Kong X, Blackman BRK, et al. Effects of impactor geometry on the low velocity impact behaviour of fibre-reinforced composites: an experimental and theoretical investigation. Appl Compos Mater 2020;27:533–53. https://doi.org/10.1007/s10443-020-09812-8.

[12] Liu H, Liu J, Ding Y, Hall ZE, Kong X, Zhou J, et al. A three-dimensional elastic-plastic damage model for predicting the impact behaviour of fibre-reinforced polymer-matrix composites. Compos Part B Eng 2020;201:108389. https://doi.org/10.1016/j.compositesb.2020.108389.

[13] Baker A, Rose F, Jones R. Advances in the Bonded Composite Repair of Metallic Aircraft Structure. 1st ed. Amsterdam: Elsevier Science; 2002.

[14] Wang CH, Doung CN. Bonded Joints and Repairs to Composite Airframe Structures. London: Academic Press; 2016. https://doi.org/10.1016/C2013-0-00565-8.

[15] Rider AN, Wang CH, Chang P. Bonded repairs for carbon/BMI composite at high operating temperatures. Compos Part A Appl Sci and Manuf 2010;41:902–12. https://doi.org/10.1016/j.compositesa.2010.03.006.

[16] Katnam KB, Da Silva LF, Young TM. Bonded repair of composite aircraft structures: A review of scientific challenges and opportunities. Prog in Aerosp Sci 2013;61:26–42. https://doi.org/10.1016/j.paerosci.2013.03.003.

[17] Kashfuddoja M, Ramji M. Design of optimum patch shape and size for bonded repair on damaged carbon fibre reinforced polymer panels. Mater and Des 2014;54:174–83. https://doi.org/10.1016/j.matdes.2013.08.043.

[18] Coelho SRM, Reis PNB, Ferreira JAM, Pereira AM. Effects of external patch configuration on repaired composite laminates subjected to multi-impacts. Compos Struct 2017;168:259–65. https://doi.org/10.1016/j.compositesb.2018.12.153.

[19] Tie Y, Hou Y, Li C, Zhou X, Sapanathan T, Rachik M. An insight into the low-velocity impact behaviour of patch repaired CFRP laminates using numerical and experimental approaches. Compos Struct 2018;190:179–88. https://doi.org/10.1016/j.compstruct.2018.01.075.

[20] Hou Y, Tie Y, Li C, Sapanathan T, Rachik M. Low-velocity impact behaviours of repaired CFRP laminates: Effect of impact location and external patch configurations. Compos Part B Eng 2019;163:669–80. https://doi.org/10.1016/j.compositesb.2018.12.153.

[21] Sun Z, Li C, Tie Y. Experimental and numerical investigations on damage accumulation and energy dissipation of patch-repaired CFRP laminates under repeated impacts. Mater and Des 2021;202:109540. https://doi.org/10.1016/j.matdes.2021.109540.

[22] Liu H, Brooks RA, Hall ZEC, Liu J, Crocker JWM, Joesbury AM, et al. Experimental and numerical investigations on the impact behaviour of pristine and patch-repaired composite laminates. Phil Trans R Soc A 2022. https://doi.org/10.1098/rsta.2021.0340. in press.

[23] American Society for Testing and Materials. ASTM D7136/D7136M. Standard Test Method for Measuring the Damage Resistance of a Fiber-Reinforced Polymer Matrix Composite to a Drop-Weight Impact Event. Pennsylvania: ASTM; 2005. https://doi.org/10.1520/D7136_D7136M-20.

[24] Dear JP, MacGillivray JH. Strain gauging for accurate determination of K and G in impact tests. J Mater Sci 1991;26:2124–32. https://doi.org/10.1007/BF00549178.

[25] Crouch BA, Williams JG. Modelling of dynamic crack propagation behaviour in the three-point bend impact specimen. J Mech Phys Solids 1988;36:1–13. https://doi.org/10.1016/0022-5096(88)90017-8.

[26] Williams JG, Adams GC. The analysis of instrumented impact tests using a mass-spring model. Int J Fract 1987;33:209–22. https://doi.org/10.1007/BF00013171.

[27] Dear JP. High speed photography of impact effects in three-point bend testing of polymers. J Appl Phys 1990;67:4304–12. https://doi.org/10.1063/1.344946.

[28] Bieniaś J, Jakubczak P, Surowska B. Comparison of polymer composites behavior to low-velocity impact and quasi-static indentation. Composites Theory and Practice 2013;13:155–9.